POLITECNICO DI TORINO
Repository ISTITUZIONALE

Experimental Demonstration of 100 Gbps/ C-Band Direct-Detection Downstream PON Using Non-Linear and CD Compensation with 29 dB+ OPL over 0 Km-100 Km

(Article begins on next page)

01 September 2025

Experimental Demonstration of 100 Gbps/λ C-Band Direct-Detection Downstream PON using Non-Linear and CD Compensation with 29 dB+ OPL over 0 km–100 km

Pablo Torres-Ferrera, Giuseppe Rizzelli, Haoyi Wang, Valter Ferrero, *Senior Member, IEEE* and
Roberto Gaudino, *Senior Member, IEEE*

Abstract—**Passive Optical Networks (PON), able to operate at 50 Gbps per wavelength (λ), are under development and standardization, based on intensity-modulation (IM) and direct-detection (DD) systems. The next step in PON evolution will be driven by 5G/6G fronthauling capacity demands, and will require the development of 100 Gbps/λ (and beyond) systems, which poses big challenges if maintaining the DD-format. In this contribution, we analyze a 100 Gbps/λ PON architecture able to preserve the IM-DD approach at the Optical Network Unit (ONU), placing the complexity at the Optical Line Terminal (OLT), thanks to Digital Signal Processing (DSP). We experimentally demonstrate a 100 Gbps/λ transmission using this architecture in the downstream (DS) direction. Chromatic dispersion digital pre-compensation (CD-DPC) in combination with an IQ Mach-Zehnder Modulator (IQ-MZM) is used at the transmitter (TX). Keeping the ONU DSP as simple as possible, as compared with current DSP proposals for 50 Gbps/λ PON, is another main goal of this work. Adaptive equalization (AEQ) is used to correct for linear impairments, in addition to digital non-linear correction (NLC) at the receiver (RX). We compare two NLC approaches: a full Volterra Non-Linear Equalizer (VNLE) and a simpler NLC technique based on a square-root like function (SQRT). Operation over standard single-mode fiber (SMF) in C-band, achieving reaches from 0 km to 100 km and Optical Path Loss (OPL) values higher than 29 dB, are shown. The analyzed proposal is directly applicable to Terabit-capable wavelength division multiplexing (WDM)-PON, and can be extended to very high-speed Time Division Multiplexing (TDM)-PON and TWDM-PON, with some modifications discussed here.**

Index Terms— **Passive Optical Networks PON, Non-linear Compensation, Chromatic Dispersion Compensation, Digital Signal Processing, 100 Gbps, PAM, Direct Detection, C-Band.**

I. Introduction

The deployment of bandwidth-hungry 5G services is driving the development of higher capacity fronthauling networks.

Every mobile phone generation typically lasts for a decade, so that the following generation 6G systems [1]-[4] will likely happen in about ten years from now, requiring even higher fronthauling data rates [3]-[5]. Regarding fixed access, all international trends show that Fiber-to-the-Home (FTTH) using PON architecture will become so widespread to be considered as a commodity in most urban areas. It is thus very likely that 6G will use the already globally deployed PON "urban web of fibers" as an underlying fronthauling infrastructure. This plausible, but not yet defined, 6G-over-optics roadmap, will require ultra-high bit rates to be handled over PON networks, since 6G will have much stronger requirements than 5G and also a stronger tendency to *cloudification* of radio-access (C-RAN). Even today, the current development of 50G-PON, the latest PON project under standardization by ITU-T targeting 50 Gbps per wavelength (λ) [6]-[8], has been driven not only by the typical fixed residential FTTH services requirements but mostly by the 5G wireless fronthauling transport ones [7]-[11]. In general, it is not yet easy to predict how much 6G will take advantage of PON, but the chances are high: 6G will not be massively deployed before 7-10 years from now, and in the meantime it is expected that PON technologies will further be deployed not only in urban environment, but also inside Office buildings (thanks to the new Fiber-to-the-Office trends) and inside production plants (see for instance [12] on industrial-PON). There could thus be in the future a perfect match between an ultra-pervasive fixed PON infrastructure and, for instance, 6G micro-cell requirements. The next step in the PON evolution, expected to target 100 Gbps/λ data rates and beyond, is already a hot research topic [5],[7],[13]-[28], which for sure will be guided by the forthcoming 6G wireless transport needs and by 6G most advance applications, like holographic telepresence or cobots [3].

In the following, we briefly review the recent evolution of PON standards towards higher bit rates, as an introduction to the core of this paper, i.e. a solution for 100 Gbps/λ PON. One constant in the PON upgrades is preserving the already installed Optical Distribution Network (ODN) infrastructure, thus guaranteeing reaches from 0 km to (at least) 20 km and an OPL of at least 29 dB. Up to now, including the recently standardized 25G-PON [29], on-off keying (OOK) modulation format has been used in combination with optoelectronic (O/E) devices

with enough bandwidth (BW). In this way, signal-to-noise ratio (SNR) penalties due to format cardinality increasing are avoided to achieve the OPL targets. To accomplish the reach target, the chromatic dispersion (CD) penalty has limited the 25G-PON operation only to O-band, in both DS and upstream (US) directions. In contrast, in all previous PON versions, the DS operation was performed in S-, C- or L-band. For 50G-PON, the same full O-band operation approach has been adopted [6]-[8]. Anyway, due to the increased data rate, some dispersion penalty becomes unavoidable, which has to be somehow compensated.

Fulfilling the OPL target is becoming challenging for 50G-PON. First, 50G-class O/E devices with enough BW for OOK operation are not yet mature, then, re-using 25G-class ones is under consideration. This bandlimited situation results in an extra power penalty, additional to the CD one, and to the SNR inherent reduction due to data rate increase. Some gain can come from increasing the TX power (P_{TX}) and from including even stronger forward error correction (FEC) to relax the BER target (BER_T) to 10^{-2} (as in 25G-PON). Moreover, the addition of digital signal processing (DSP), for the first time in PON, to counteract some CD and O/E BW limitations, has been widely proposed [7],[30]-[34].

The situation becomes even more critical when, as likely required by future 6G fronthauling, PON will target 100 Gbps/λ (100G-PON) and beyond. In these conditions, several works have proposed to move from the traditional DD systems to the coherent ones [22]-[28], in order to gain in sensitivity and CD resilience. Using DSP-based CD compensation [22], [24], [28], allowed "inherently" in coherent PON, would permit to enable again S/C/L-band operation. This has the advantage of incurring in less fiber losses, and operating in a window forecasted to get free after future service migration to 25G- and 50G-PON [18], [27], both fully operated in O-band. However, a PON system is especially sensitive to cost, complexity and power consumption in the ONU side. Therefore, the use of coherent technology, even with reduced complexity, is still under discussion [13], [14], [28], being one of its main problems the need of ultra-stable narrow linewidth lasers, which are costly for the moment.

One alternative for C-band 100G-PON, able to keep the DD scheme and the ONU complexity similar to that of some proposals for 50G-PON (i.e., re-using 25G-class O/E and including reasonable simple DSP [7], [8]), was proposed by our group in [18], extending a previous similar proposal for 50G-PON [35]. To re-use 25G-class devices, PAM-4 is proposed as modulation format, counteracting the corresponding power penalty with respect to OOK by a higher transmitted power [13], [36], [37] and integrating SOA pre-amplification at RX [14], [37]-[40]. The price to pay to keep the ONU simple, in such a very demanding 100G-PON environment, is concentrating the complexity in the OLT. This means, placing a complex transmitter (receiver) in the OLT for the DS (US) direction (see Fig. 1(c)). The following combinations can achieve these goals.

i) For the DS in C-band: an IQ-DD MZM in combination with CD-DPC is used at the TX-OLT, and DD including DSP-AEQ is used at the RX-ONU as in [18].

ii) For the US in C-band: a PAM-4 intensity modulator (IM) is used at the TX-ONU, and a coherent receiver as in [24]-[27], or DD plus Machine Learning (ML) DSP as in [19], [20], is used at the RX-OLT.

iii) For the US in O-band: a PAM-4 intensity modulator (IM) is used at the TX-ONU, and a DD with DSP-AEQ is used at the RX-ONU, as in [14]-[17].

These options do not consider the issue of backward wavelength compatibility with previous PON standards. In fact, considering all ITU-T and IEEE standards released up to now, the PON spectrum is basically full, so that likely the next-generation PONs will have to be placed on top of some of the previously standardized bands, but this problem is outside the scope of our paper.

We have previously analyzed by means of simulations and experiments the system referred in point (*i*) for the DS direction, shown in Fig. 1(a), for fiber lengths of 25 km and 50 km [18]. In this new contribution, we further elaborate over this proposal, by largely extending our analysis in these directions:

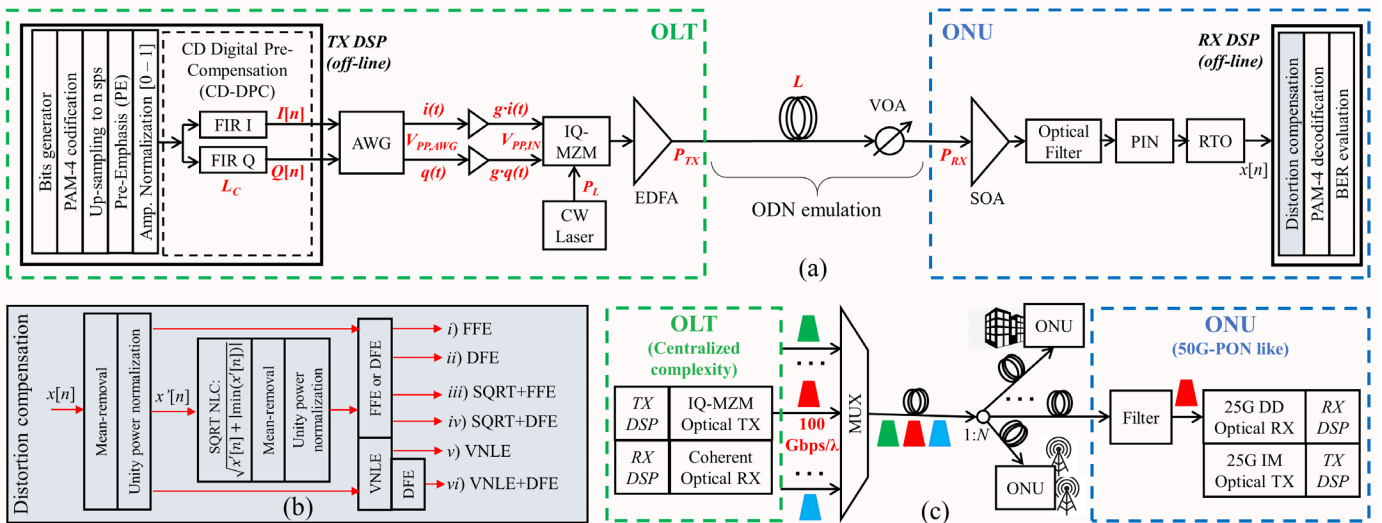Fig. 1 a) Experimental setup of the CD-DPC and DD analyzed system, emulating a PON downstream transmission; b) Distortion compensation blocks used at the RX side, showing the different DSP options; c) WDM-PON simplified scheme of a Terabit-capable system centralizing the complexity at the OLT side to maintain an IM-DD ONU with 50G-PON-like DSP complexity. The downstream direction is shown in the figure.

1. Including fiber lengths inside the standard range of PON (0 km–20 km) and even extended reaches up to 100 km.

2. Including RX non-linear compensation (NLC), in particular a relatively simple technique proposed in [41], [42], compared against a more complex Volterra Non-Linear Equalizer (VNLE), used as an upper-boundary reference (see Fig. 1(b)).

3. Discussing PON solutions directly based on our proposal, such as WDM-PON, and possible adaptations to operate also under TDM-PON and TWDM-PON conditions.

Moreover, in addition to the discussion about specific applications of the system under analysis, we present a vast set of experimental results, varying key design parameters, which provide technical insights of the impact of non-linear distortion (and its compensation) on CD pre-compensated systems. Since the ideal CD pre-compensation functionality relies on the assumption of linear (and thus exchangeable) system elements, inserting non-linearity in such kind of system produces penalties and trade-offs worth to be investigated.

The paper is organized as follows. In Section II, we describe the possible next-generation PON applications that motivates and justify our contribution. In Section III, we state the main details of our experimental setup. In Section IV, experimental results are reported, analyzed and discussed. We conclude summarizing our main findings in Section V.

II. PON APPLICATIONS OF THE ANALYZED SYSTEM

During the development of Next Generation PON (NG-PON2), different PON architectures were proposed in IEEE and ITU-T to achieve the 40 Gbps rate target: WDM-PON, TDM-PON and TWDM-PON [8], [34], [43]. One of the finally standardized solutions in ITU-T G.989 is a point-to-point WDM-PON overlay (PtP WDM-PON) which was meant to provide high-data rate services by dedicating one λ to each ONU [43] (see Fig. 1(c)). For 25G-PON and 50G-PON, the TDM-PON architecture was preferred. In recent years, at the research level, and driven by the current 5G and future 6G wireless transport increase bit rate requirements, WDM-PON has been found to be a promising technology to enable high capacity and low latency cells interconnection due to its dedicated wavelength scheme [5],[7],[9],[44],[45]. In addition, from an operational point of view, WDM-PON network management is simpler than TDM-PON [9]. Based on 5G fronthaul network requirements, WDM-PON operation with at least 25 Gbps/λ capacity is expected to be needed [9], [44], whereas higher 6G data rates [3], [46] will demand for terabit-capable WDM-PON with increasing capacity per λ, such as 100 Gbps/λ [5],[44],[45].

As mentioned in previous section, achieving such a high single-λ data rate is challenging using DD. Very high capacity DD systems transmitting up to 440 Gbps/λ using complex DSP, single-side band optical modulation and Kramers-Kronig RX, have been reported for data-center interconnections (DCI) [47]-[49]. However, for the PON realm (i.e. higher OPL target than in DCI), state-of-the-art DD proposals remain around the 100 Gbps/λ transmission [14]-[22].

A C-band 100 Gbps/λ WDM-PON architecture, able to keep an IM-DD ONU by centralizing the complexity at the OLT (shared-element), is shown in Fig. 1(c). For the US direction, an IM TX plus a coherent RX has been shown feasible and studied in detail in [24]. The less explored DS ingredient, using DD at the ONU, has been analyzed by our group in [18] and is extended in the present contribution. Our proposal is focused on sticking with DD, but obviously needs to add complexity compared to the current 50G-PON solutions. In particular, it requires in the central office an IQ-modulator (of the same complexity as those used for advanced coherent transmission but on a single polarization) and DSP algorithms to perform CD-DPC. Basically, our proposal is based on a field-level modulation, through an IQ-modulator, driven by two DSP-based pre-computed Finite Impulse Response (FIR) filters that emulates the inverse of the link accumulated dispersion. Consequently, the OLT distance to the target ONU, i.e. the target L, should be known in advance with a reasonable accuracy to set the proper pre-compensated length (L_C) at the CD-DPC block. A mismatch between L and L_C ($\Delta L = L - L_C$) of few kilometers (around ±2 km [18]) can be tolerated. Then, it is not immediately applicable to TDM-PON, where the target distances between the OLT and a set of ONUs can be from 0 km to 20 km. Conversely, it is directly feasible for PtP WDM-PON, since a continuous transmission, using a dedicated λ, is performed between the OLT and each ONU, thus being able to properly fix the L_C and the corresponding CD-DPC configuration.

Some possibilities to adapt our proposal to TDM-PON were discussed in [18], based on using dynamic FIR filters able to reconfigure its taps inside a frame depending on the OLT-ONU$_i$ target distance, as shown in Fig. 2. In light of the new
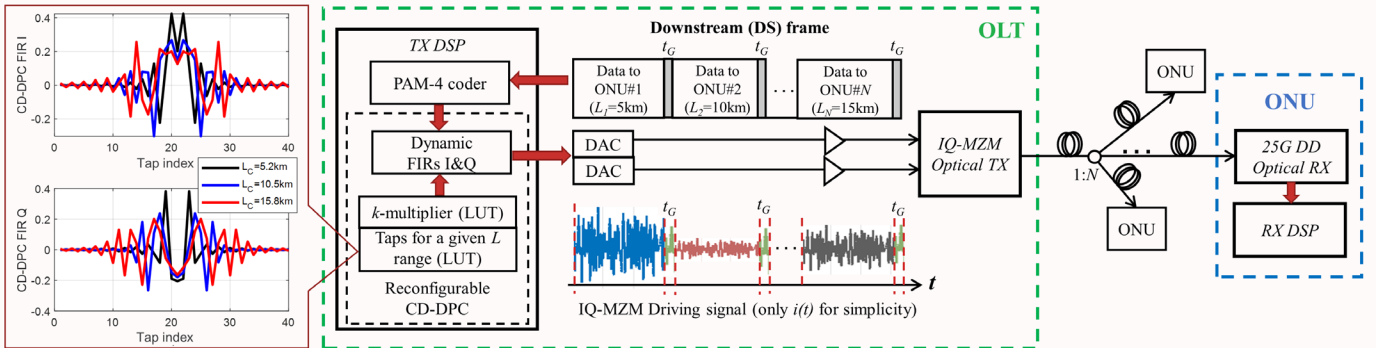

Fig. 2 TDM-PON adaptation based on the CD-DPC TX + DD RX approach shown in Fig. 1(a). The TDM-PON adaptation requires dynamic FIRs able to change their taps inside a DS frame, depending on the L target of the corresponding ONU data, reading them from a Look-Up Table (LUT), which is more complex from a system operation point of view but still possible from a technical one. Left-sided: Tap coefficients of the CD-DPC block for three pre-compensated lengths L_C before multiplying the coefficients by a given scalar k-factor to optimize the amplitude of the driving signals for each fiber length L target.

experimental results reported in the present contribution, we are able to extend and support this discussion. Here, we experimentally tested L values inside the typical PON range, covering operation from 0 km to 20 km, as shown in sub-section IV.B. Different sets of CD-DPC taps were used for each target L, showing correct operation in all cases (we tested L = 5.2 km, 10.55 km and 15.8 km, for lab inventory availability). These set of taps can be stored in a Look-Up Table (LUT) for few different L_C values. Then, the FIRs coefficients are loaded from the LUT, choosing the proper set of taps depending on the L-target. A range of physical lengths around a given L_C will use the same taps, choosing this range inside the feasible ΔL tolerance, as detailed in sub-section IV.B.

Moreover, a mixed TWDM approach can be used, simplifying the operation scheme. The ONUs can be grouped in few subsets (i.e., 3 or 4) depending on their distance to the OLT, and a single-λ can serve them all, setting the same pre-compensated length L_C at the OLT. A proper grouping should guarantee that all the OLT-ONU distances, in each ONU subset, are inside the ΔL tolerance of the system. Then, the TDM approach can be performed inside the ONU subset, without requiring any other system adaptation.

Regarding the considered multi-λ options, we focus only on the splitter-based PON architecture. Today, this is the only massively deployed PON solution and most operators worldwide are interested just in this option. Our proposal would anyway also be applicable to array waveguide grating (AWG)-based PON architectures (i.e. solutions using a WDM multiplexer instead of the splitter), but this option is not further investigated in the rest of the paper. An optical filter is then needed in the proposed SOA pre-amplified receiver (See Fig. 1.c). Its characteristics (and thus cost/complexity) would depend on the application scenario. For single-λ 100G-PON, it can be a filter with relaxed tolerances, mostly to reject SOA ASE noise. For multi-λ operation, it should be similar to the ones envisioned for ITU-T G.989 NG-PON2, i.e., narrow and possibly tunable filters.

By taking advantage of the CD-DPC functionality, the PON reach can also be extended beyond 20 km. In this paper, we experimentally show successful C-band operation over 25.23 km, 50.46 km, 81.1 km and 106.2 km of standard SMF, achieving more than 29 dB of OPL in all cases. From a possible application point of view, up to 50 km reach is required by the recent Super PON proposal [50], [51] and similar long-reach PON [52], [53] alternatives. Our analysis for L > 50 km, i.e., 81.1 km and 106.2 km, is not intended for a practical PON system, since due to the high total fiber loss there is not enough power budget margin for splitter and connectors. Instead, we perform this analysis to explore the fiber length tolerances of a high-rate CD-DPC system and to forecast technical features when using higher data rates. For instance, considering a bit rate doubled to 200 Gbps, the tolerance to dispersion is reduced four times, so the reported dispersion penalty of 80 km and 100 km for 100 Gbps would be similar to that of 20 km and 25 km for 200 Gbps, fiber lengths close to the standard PON reach targets.

In summary, the proposal analyzed in this contribution is the downstream ingredient of a Terabit-capable PON solution for future 5G/6G transport able to operate over several wavelengths in the C-band. Moreover, the ONU receiver complexity is kept

close to the one projected for some advanced current 50G-PON transceiver proposals.

III. EXPERIMENTAL SETUP

Our experimental setup is shown in Fig. 1(a). At the TX DSP, a random PAM-4 sequence, 2^{15}-1 bits long and repeated several times, is off-line generated and processed. An equispaced PAM-4 eye is set since optimizing the PAM-4 levels was shown to give negligible advantages when RX-NLC is applied [54]. The 100 Gbps PAM-4 sequence is then up-sampled to 1.82 samples per symbol (SpS), to match the fixed sampling frequency of 92 GS/s in the arbitrary waveform generator (AWG) available in our lab. In our DSP, we also inserted a simple frequency pre-emphasis (PE) block to partially pre-compensate for electronic bandwidth limitations. This PE is an inverse low-pass one-pole filter with optimized -3dB frequency f_P, and a steep cut-off for frequencies higher than the baud rate. The resulting signal is normalized and filtered by the CD-DPC block, described in detail in [18]. Different pre-compensated lengths L_C were set depending on the L target. According to simulations [18], 40 and 160 CD-DPC taps were enough for target L's lower and higher than 100 km, respectively. To be on the safe side, we set 320 taps for L = 106.2 km, and 80 taps for the rest of the L's.

The CD-DPC output real-valued signals $I(n)$ and $Q(n)$ are digital-to-analog converted by the AWG and electrically amplified to generate the signals that drive the 25G-class IQ-MZM. The modulator I and Q arms are biased around quadrature and null point, respectively. The central lambda of the CW laser is 1549 nm. Different driving signal amplitudes ($V_{PP,IN}$) where tested, to analyze the trade-off between the modulator non-linearity and optical modulation index (OMI), which depend on this $V_{PP,IN}$ key parameter.

After the IQ-MZM, an EDFA amplifies the optical modulated signal launched into the fiber. The average transmitted power P_{TX} is set equal to ~11 dBm, which would actually be reachable also with a booster SOA [36], [37]. We used an EDFA only because we did not have a suitable booster SOA in our lab. Conventional ITU-T G.652 SMF fibers with L = 0.001 km (a patch-cord for optical back-to-back (BtB) benchmarking), 5.2 km, 10.55 km, 15.8 km, 25.23 km, 50.46 km, 81.1 km and 106.2 km, are used. At the fiber output, a variable optical attenuator (VOA) sets the OPL, evaluated (in dB) as the difference between the average P_{TX} (in dBm) and the average received optical power (ROP, in dBm). A pre-amplifier SOA, a 10-nm optical filter, and a broadband PIN+TIA compose the optical DD RX.

The PIN+TIA output signal is analog-to-digital converted and stored using a 200 GS/s real-time oscilloscope (RTO). The digitized sequence is down-sampled and off-line processed at 2 SpS (i.e. at 100 GS/s), using one of the six DSP distortion compensation options shown in Fig. 1(b) and described in the following:

i) An adaptive half-rate feed-forward equalizer (FFE) with N_{FF} taps: FFE(N_{FF}).

ii) An adaptive half-rate decision-feedback equalizer (DFE) with N_{FF} taps and N_{FB} taps in the feed-forward and feedback

sections respectively: DFE(N_{FF},N_{FB}).

iii) A square-root like (SQRT) block [41], [54] detailed in Fig. 1(b), followed by an FFE(N_{FF}).

iv) A SQRT block followed by a DFE(N_{FF},N_{FB}).

v) A third-order half-rate VNLE with 121 linear memory and 5 cubic and quadratic memory.

vi) The same VNLE as (*v*), followed by a DFE(20,5) block.

Unless otherwise stated, N_{FF} = 120 taps and N_{FB} = 5 taps. All the AQE are operated in full-training mode. A marginal penalty was verified when switching the equalizers to tracking-mode after a long-enough training stage and proper tracking step-size adaptation coefficient μ selection. All the AEQ use the least-mean square (LMS) algorithm for taps adaptation. After distortion compensation, the PAM-4 RX sequence is decoded by minimum distance algorithm and the BER is evaluated through direct error counting over ~10^6 bits.

IV. EXPERIMENTAL RESULTS

In this Section, we report the results obtained using the setup shown in Fig. 1(a) after a vast experimental campaign. As a starting point, we show the BtB performance, then we continue analyzing the system performance for fiber lengths inside the typical PON ranges, and finally for extended reaches. We focus our attention in the comparison between results using DSP without direct NLC, including SQRT NLC and using the more complex VNLE NLC as an upper-bound performance estimator. In addition, the mismatch tolerance between pre-compensated length L_C and fiber length target L is analyzed. Finally, we discuss the performance degradation as a function of L, and the receiver DSP complexity.

A. Back-to-back characterization

The IQ-MZM driving signals peak-to-peak amplitude ($V_{PP,IN}$, measured in the In-phase component) is a parameter to be optimized. Increasing $V_{PP,IN}$ results in a higher OMI, but also higher modulator non-linearity. Including a form of NLC allows to increase the OMI, thus improving the performance.

A collection of BER versus OPL data was obtained for different $V_{PP,IN}$ values, from which the achievable OPL that guarantees the $BER_T = 10^{-2}$ is evaluated. The CD-DPC block is turned off in BtB. In Fig. 3, we plot BER versus OPL curves, setting the optimum $V_{PP,IN}$ value for each curve and comparing different DSP approaches. In Fig. 4, we plot the achievable OPL as a function of $V_{PP,IN}$, displayed normalized with respect to the IQ-MZM bias V_π.

From Fig. 3 and Fig. 4, we can observe the advantages of including NLC techniques. A 0.6 dB and 0.8 dB gain is obtained thanks to the SQRT NLC and VNLE, respectively, for a $BER_T = 10^{-2}$. In Fig. 3, it is shown that this gain increases when decreasing the BER_T. In the rest of the manuscript all the power gains/penalties are referred to a $BER_T = 10^{-2}$, the pre-FEC BER_T considered in 25G- and 50G-PON. The gain provided by DFE is very small in all cases (<0.1 dB), especially when combined with VNLE (in this case it becomes negligible). A 0.15 dB penalty is observed when reducing the number of FFE taps from 120 to 20 taps in the SQRT+FFE approach. These results indicate that the system in BtB is not strongly bandlimited.

From Fig. 4, we can observe that in BtB, all the DSP options obtain similar performance for low values of $V_{PP,IN}$. The curves

split apart when increasing $V_{PP,IN}$, showing an increase in the NLC gain. These facts indicate that, in BtB, the more important source of system non-linearity is the IQ-MZM, due to the well-known *sin-like* input-output relation of the MZM. Moreover, the optimum $V_{PP,IN}$ value is higher when including the SQRT-NLC, and even higher when including a VNLE. Therefore, the NLC schemes effectively allow an OMI increase, thus improving the performance, being VNLE the most powerful approach, as expected.

The achievable OPL values obtained in BtB (for optimum $V_{PP,IN}$), of at least 34 dB using the simpler DSP alternatives, indicate that there is at least a 5-dB margin to allow for fiber propagation penalties and/or transmitted power reduction.

B. Standard-reach PON lengths

In this sub-section, we analyze the system using three fiber lengths inside the standard reach for PON (up to 20 km): 5.2 km, 10.55 km and 15.8 km. When including the SMF, apart from the non-linear Kerr effect, the introduction of CD in combination with DD generates another source of non-linear distortion. According to [41], the simple SQRT NLC module can help on compensating for it.

The previous analysis performed in BtB is repeated for L = 15.8 km. The pre-compensated length was set L_C = 14.8 km (since Kerr effect compensates for some CD, the optimum L_C is lower than L [18]). Fig. 5 shows achievable OPL curves as a function of the normalized $V_{PP,IN}$. We can observe that, when including the 15.8 km SMF, the NLC gain is higher, while the advantage of including DFE is as small as in BtB. A 3-dB difference between the best FFE operation and the best VNLE one is observed. A lower, but still significant, 1.3 dB gain is measured when including the SQRT NLC to FFE or DFE, and setting the optimum amplitude in each case. This gain can be even larger if setting the same driving signals amplitude, for instance: equal to 1.8 dB for a $V_{PP,IN} \sim 0.3 \cdot V_\pi$. A slightly higher penalty of 0.3 dB as compared to BtB, when reducing the FFE taps from 120 to 20 is observed. This means that FFE is slightly correcting for fiber penalties.

A comparison between the achievable OPL of BtB and L = 15.8 km cases shows that the best VNLE performance in both cases is the same. Therefore, VNLE is correcting for almost all
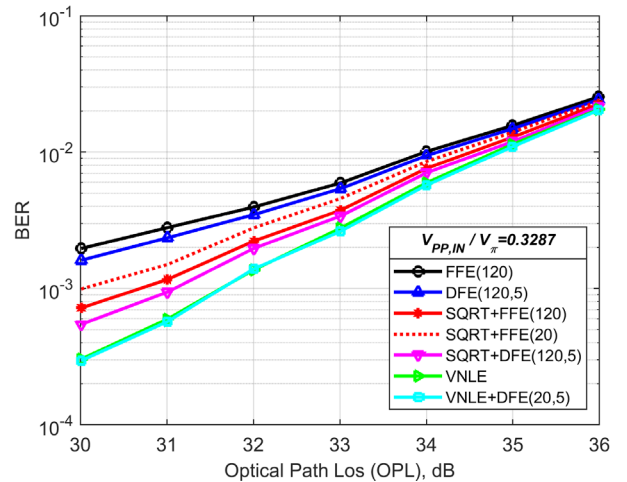

Fig. 3 BER as a function of the OPL in BtB configuration setting the optimum amplitude of the IQ-MZM driving signals. Different DSP distortion compensation options are compared.
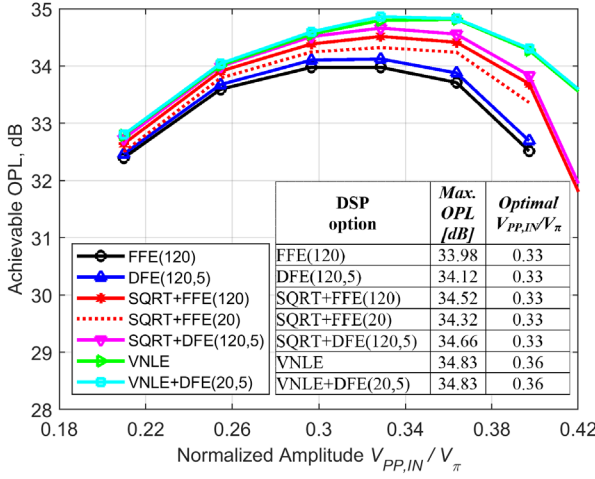
Fig. 4 Achievable OPL to fulfill the $BER_T = 10^{-2}$ in BtB as a function of the peak-to-peak in-phase signal amplitude $V_{PP,IN}$ at the modulator input normalized to the modulator bias V_π, comparing different DSP options. Inset: table showing the maximum OPL and optimal amplitude for each DSP option.
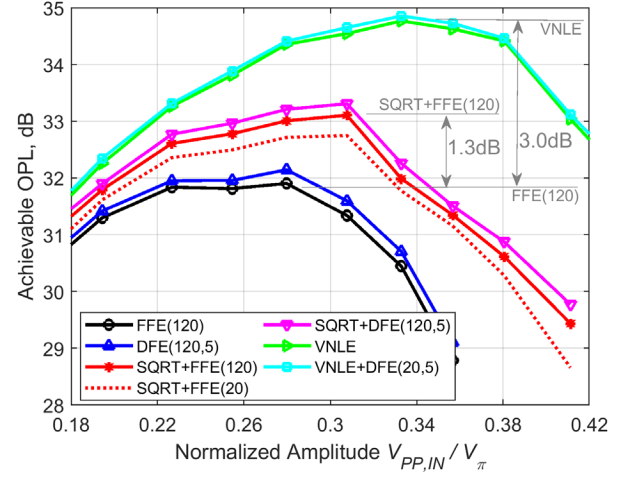

Fig. 5 Achievable OPL to fulfill the $BER_T = 10^{-2}$ for $L = 15.8$ km as a function of the peak-to-peak in-phase signal amplitude $V_{PP,IN}$ at the modulator input normalized to the modulator bias V_π, comparing different DSP options. Best performance difference between some DSP options are indicated.

the non-linear distortions generated by including the 15.8 km SMF. We can then attribute a 2-dB non-linear penalty to the 15.8 km SMF addition: the difference between the 34 dB (see Fig. 4) and the 32 dB (see Fig. 5) achievable OPL obtained in BtB and 15.8 km cases, respectively, using FFE alone.

A reduction of the optimum normalized $V_{PP,IN}$, when including the SMF in comparison with BtB, can be observed for the DSP options without NLC (i.e. FFE and DFE). Simulations anticipated this in [18], and experimental results shown here confirm it. This fact is due to the use of CD-DPC, whose effectiveness relies on the linearity of the blocks, so that they are exchangeable without penalty. Thus, when including CD-DPC, a lower degree of non-linearity can be tolerated. If using VNLE, the optimum $V_{PP,IN}$ remains practically the same when comparing the BtB and the 15.8 km cases. This fact confirms the good degree of non-linear correction achieved by this equalizer. Similar results were obtained for the other two tested fiber lengths (not shown here due to space limitations).

The previously discussed results were performed for a single fiber length L and a single pre-compensated length L_C.

To analyze the TDM-PON extension discussed in Section II, feasible operation over different fiber lengths using the same L_C should be demonstrated. In addition, the full 0 km to 20 km range should be covered, by just pre-evaluating 3 or 4 sets of CD-DPC taps corresponding to 3 or 4 L_C values properly distributed. Due to inventory limitations in our lab, we followed a different, but equivalent approach (under linear conditions both approaches are identical): we fixed three physical fiber lengths ($L = 5.2$ km, $L = 10.55$ km and $L = 15.8$ km), and then we changed the pre-compensated lengths L_C around these L values. For each combination of L and L_C we obtain a set of curves as those presented in Fig. 5, from which we can extract the maximum achievable OPL using the optimum $V_{PP,IN}$, for each DSP approach. In Fig. 6, we show the obtained achievable OPL values as a function of L_C, for three fiber lengths: 5.2 km (dotted lines), 10.55 km (dashed lines) and 15.8 km (solid lines). Since DFE was shown to provide small advantage for these L values, we display only the FFE and VNLE approaches.

From Fig. 6 we can observe that by using VNLE, the 0 km – 20 km range can be covered by properly adjusting the CD-
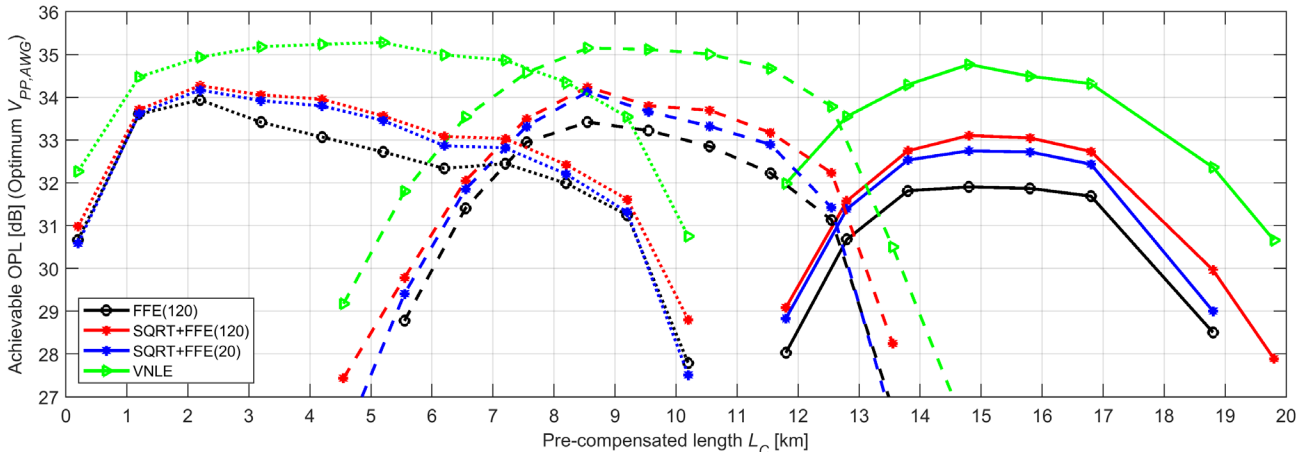

Fig. 6 Achievable OPL to fulfill the $BER_T = 10^{-2}$ as a function of the pre-compensated length L_C set at the CD-DPC block, for three L targets of 5.2 km (dotted lines), 10.55 km (dashed lines) and 15.8 km (solid lines). The tolerance to the mismatch between L and L_C is shown (for each L target). The optimum amplitude of the IQ-MZM driving signals is set for each L target and pre-compensated fiber length L_C. Different DSP distortion compensation options are compared.

DPC taps depending on the L range of operation, achieving an OPL higher than 30 dB. However, a full VNLE is a very complex solution to use in the ONU. In contrast, the SQRT-NLC technique is simpler and still can provide a gain in the full range against FFE alone. This gain is higher (1.0-1.6 dB) for the longer fiber lengths range: 13 – 20 km. Over this range the non-linear penalty increases, as shown by the ~2-dB performance reduction, as compared to BtB, when using FFE alone. Using the SQRT+FFE(120) option, an OPL ≥ 29 dB can be achieved in the $L = 0 – 19$ km range. If the FFE taps are reduced from 120 to 20, this range is only reduced by 1 km to $L = 0 – 18$ km. Therefore, the SQRT+FFE(20) option can be a feasible solution when operating inside the standard range for PON, whose complexity (see Table I) is comparable to the DSP options currently assumed for 50G-PON [7], [8], [38].

C. Extended-reach PON

As mentioned in Section II, the use of dispersion pre-compensation allows extending the system reach beyond 20 km, even in C-band. In this sub-section we analyze operation over fiber lengths $L = 25.23$ km, 50.46 km, 81.1 km and 106.2 km. We start the analysis for $L = 50.46$ km, a target distance that has been considered for Super PON and other similar Long-Reach PON scenarios [50]-[53].

In Fig. 7, the achievable OPL as a function of the normalized $V_{PP,IN}$ is shown for $L = 50.46$ km and $L_C = 47.46$ km. A performance degradation with respect to the BtB (see Fig. 4) and 15.8 km (see Fig. 5) cases can be observed, even when using VNLE. A 1.6 dB penalty is measured for 50.46 km with respect to BtB using VNLE. The optimum $V_{PP,IN}$ is shifted to lower values, as compared to BtB, following the trend discussed in sub-section IV.B. For $L = 50.36$ km, this occurs also when using VNLE. Therefore, a strong non-linear distortion, arising from including the 50.46 km SMF, is present, and the VNLE cannot fully compensate it, as it does for shorter SMFs (as shown for 15.8 km). The VNLE order and/or memory should then be increased to enhance its performance at these fiber lengths.

A power penalty with respect to VNLE of 2.1 dB and 0.9 dB is obtained when using FFE alone and SQRT NLC, respectively. DFE provides a slightly higher gain (~0.3 dB) as for BtB and shorter lengths. The penalty produced by reducing the FFE taps in the SQRT+FFE approach is significant: 0.8 dB and 2.3 dB when reducing from 120 to 40 and 20 taps, respectively (see also Figures 9 and 10).

In Fig. 8, the achievable OPL as a function of L_C is shown, for a fiber length of 50.46 km. The optimum $V_{PP,IN}$ is set for each L_C value. A reduced tolerance to ΔL with respect to shorter fiber lengths (see Fig. 6) is observed, which is around ±2 km for a 1-dB penalty. From this graph, we can observe that DFE can contribute to enlarge the tolerance to ΔL. More than 29 dB OPL can be achieved, provided the proper L_C is set, even with the simpler DSP approaches, but with a reduced ΔL margin. Then, a PtP WDM-PON operation based on our proposal is more suitable than TDM- or TWDM-PON at such long distances. Note that the difference between L and the optimum L_C is higher (but still optimum $L_C < L$) as compared to shorter distances, confirming our explanation of this phenomenon attributed to the interaction between Kerr effect and dispersion. Similar trends can be observed for the other analyzed fiber lengths (not shown here due to space limitations).

From the curves of OPL vs. L_C as those shown in Figures 6 and 8, we can extract the maximum achievable ODN loss for every L target, corresponding to the optimum L_C, for each DSP approach. This information is presented in Fig. 9, which summarizes the results presented here by showing the maximum OPL values at every length experimentally analyzed: $L = 0.001$ km (BtB), 5.2 km, 10.55 km, 15.8 km, 25.23 km, 50.46 km, 81.1 km and 106.2 km. From Fig. 9, a performance drop is observed for fiber lengths higher than 10 km, except when using VNLE. Then, we can attribute this behavior to non-linear distortion due to the fiber. After 16 km (50 km in the case of VNLE), a smoother power degradation is observed up to 100 km. The steepness is not completely zero, since both dispersion and non-linear distortion are not completely compensated. Note
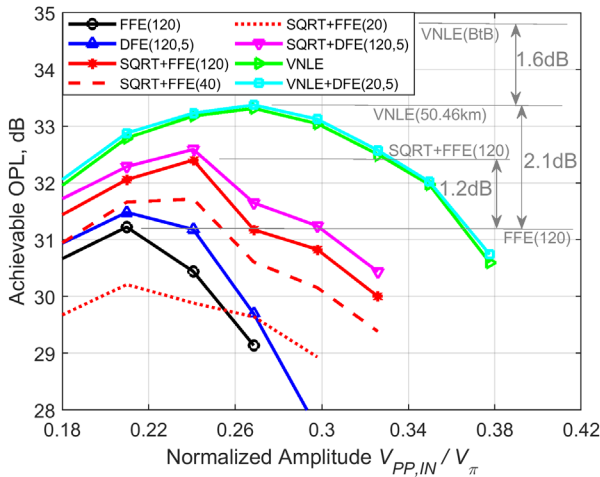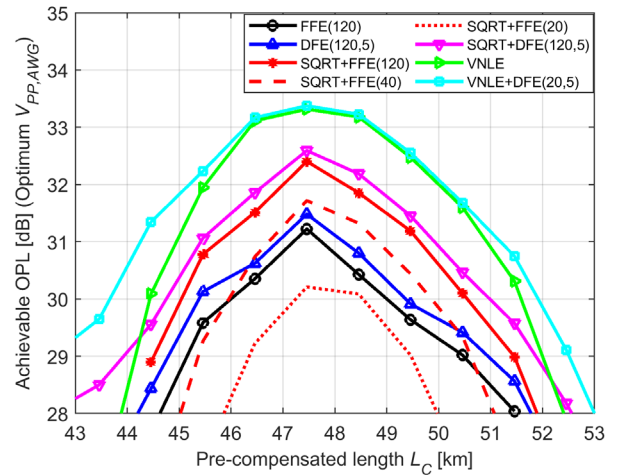

Fig. 7 Achievable OPL to fulfill the $BER_T = 10^{-2}$ for $L = 50.46$ km as a function of the peak-to-peak in-phase signal amplitude $V_{PP,IN}$ at the modulator input normalized to the modulator bias V_π for different DSP distortion compensation (see Fig. 1(b)). The CD-DPC pre-compensated length was set $L_C = 47.46$ km. Best performance difference between some DSP options are indicated.

Fig. 8 Achievable OPL to fulfill the $BER_T = 10^{-2}$ as a function of the pre-compensated length L_C set at the CD-DPC block, for $L = 50.46$ km. The tolerance to the mismatch between L and L_C is shown (for each L target). The optimum amplitude of the IQ-MZM driving signals is set for each L target and pre-compensated fiber length L_C. Different DSP options are compared.
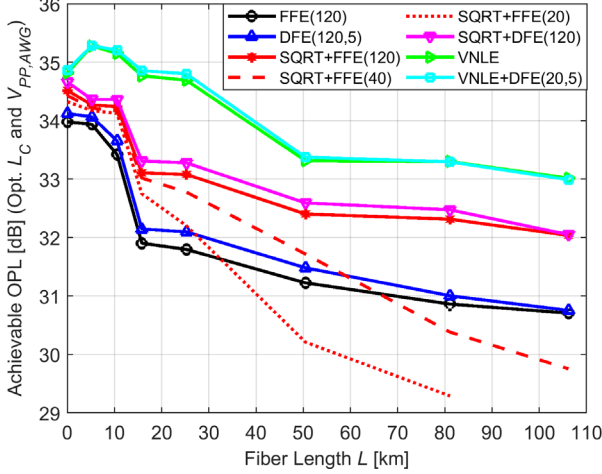
Fig. 9 Maximum Achievable OPL to fulfill the $BER_T = 10^{-2}$ as a function of the target fiber length L. The optimum L_C and amplitude of the IQ-MZM driving signals is set for each L target. Different DSP options are compared.

that the CD-DPC operates using FIRs with finite number of taps, and the memory of the non-linear terms of VNLE is also finite.

The achievable OPL, using optimum parameters and long-enough equalizers, is higher than 29 dB over the full 0 km -100 km range, which gives some margin to reduce the transmitted power by a couple of dBs, from 11 dBm to a more practical value of 9 dBm [37], [38]. A reduction in the number of FFE taps in the SQRT+FFE approach (from 120 to 40 or 20), produces a small penalty for fiber lengths shorter than 15 km, and a sharp performance reduction for larger distances.

D. Receiver DSP Complexity

In order to further analyze the impact of simplifying the SQRT+FFE scheme by reducing the FFE number of taps, in Fig. 10 we plot the achievable OPL as a function of this parameter, for three distances $L = 15.8$ km, 25.23 km and 50.46 km. The L_C and $V_{PP,IN}$ parameters are the optimum ones for each L. A marginal penalty can be observed if reducing the taps from 120 to 60 for distances equal or shorter than 50 km. As shown
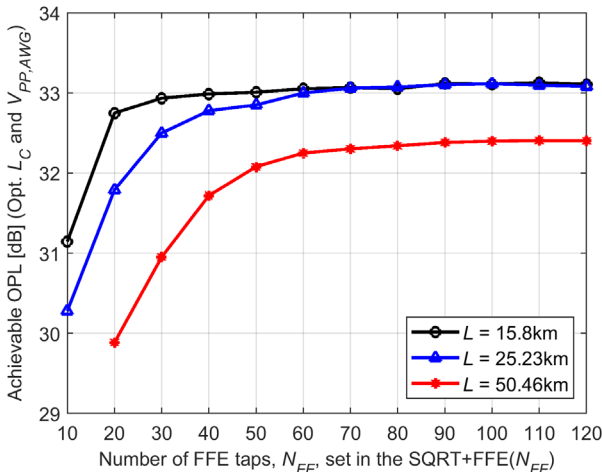

Fig. 10 Maximum Achievable OPL to fulfill the $BER_T = 10^{-2}$ as a function of the number of taps of the FFE equalizer, for three L targets. The SQRT+FFE(N_{FF}) DSP approach is used. The optimum L_C and amplitude of the IQ-MZM driving signals is set for each L target.

TABLE I. MULTIPLICATIONS PER SAMPLE (*MPS*) OF THE DIFFERENT RECEIVER DSP OPTIONS SHOWN IN FIG.1B

DSP option	*MPS*	Note
FFE(120)	120	$MPS = N_{FF}$
DFE(120,5)	125*	$MPS = N_{FF}+N_{FB}$
SQRT+FFE(20)	22	SQRT implemented as a 2nd order polynomial function as in [54], thus requiring two extra *MPS*.
SQRT+FFE(120)	122	
SQRT+DFE(120,5)	127*	
VNLE	256	VNLE multiplications per sample evaluated as in [55].
VNLE+DFE(20,5)	281*	

* Note: DFE requires additional implementation complexity due to the need of a feedback path.

before, 20 FFE taps would be enough for operation inside the 0 km – 20 km typical PON range. Note that this system is operated in C-band. Thus, achieving 100 Gbps/λ transmission (OPL ≥ 29 dB) with a DD RX plus FFE using only 20 taps, confirms the correct operation of the CD-DPC at the TX and the SQRT NLC at the RX.

Finally, to compare the complexity of the DSP options considered at the receiver, we select the metric multiplications per sample (*MPS*). In the case of FIR filters, the *MPS* are equal to the number of taps. Therefore, for FFE and DFE, the *MPS* = N_{FF} and *MPS* = $N_{FF}+N_{FB}$, respectively. It is a well-known fact that the implementation of DFE further increases the complexity due to the need of a feedback path. Regarding VNLE, a formula to evaluate the *MPS* is reported in Eq. 5 of [55], as a function of the VNLE order (here equal to 3), and the memory per kernel (here equal to 121 for the linear part, and 5 for the quadratic and cubic ones). The number of VNLE *MPS*, corresponding to the values used in this work, is 256. Finally, the SQRT-NLC can be implemented using a Look-Up Table (LUT), or approximating the SQRT function to a second-order polynomial function (POLY), as described in [54]. In [54], it is shown that the performance of SQRT and POLY is practically identical. Therefore, the number of *MPS* of SQRT implemented as a quadratic polynomial is only two. In Table I, we show a summary of the previous complexity discussion, including the actual number of *MPS* of the compared DSP options with the parameters used here.

V. Conclusion

We experimentally extended the analysis of the downstream path of a 100 Gbps/λ PON proposal, operating in C-band, able to keep the DD scheme at the RX (ONU) side. Apart from CD pre-compensation, we introduce a SQRT NLC block which was compared against a full third-order VNLE. This SQRT technique, in top to a FFE(20), has around 10x less complexity, measured as required multiplications per sample, than the full VNLE. Yet, a gain between 1.0 – 1.6 dB is provided by adding the SQRT NLC in top of FFE or DFE, allowing feasible operation (i.e., OPL > 29dB) over different fiber distances from 0 km to 100 km.

A negligible penalty with respect to BtB is obtained when using CD-DPC and VNLE, for fiber lengths from 0 to at least 25 km. For longer reaches, up to at least 100 km, a maximum penalty of 2 dB is measured. This penalty is attributed to the use of VNLE with finite order and memory and CD-DPC with finite number of taps. In comparison, when using CD-DPC and FFE or DFE alone, without any NLC block, a 2-dB penalty is

obtained after ~15 km, which increases to 3.2 dB for a 100 km reach.

A combination of CD-DPC, SQRT NLC and FFE with 20 taps provides an OPL > 29dB inside the standard PON reaches (0 km to 20 km) in C-band, keeping the DD scheme and reasonable DSP complexity at RX side. Therefore, the previous architecture represents a straight-forward proposal for future high-speed PON systems able to fulfill the forecasted very demanding 6G capacity requirements.

A single-λ transmission was here investigated. However, the analyzed system has the potential to be the ingredient of a very high-speed multi-λ system, for instance, under the TWDM or WDM schemes. An experimental verification of our proposal in a multi-λ scheme is an open research topic to be studied in the near future.

REFERENCES

[1] W. Jiang, B. Han, M. A. Habibi and H. D. Schotten, "The Road Towards 6G: A Comprehensive Survey," in IEEE Open Journal of the Communications Society, vol. 2, pp. 334-366, 2021.
[2] C. D. Alwis, et al., "Survey on 6G Frontiers: Trends, Applications, Requirements, Technologies and Future Research," IEEE Open Journal of the Communications Society, vol. 2, pp. 836-886, 2021.
[3] I. Tomkos, D. Klonidis, E. Pikasis and S. Theodoridis, "Toward the 6G Network Era: Opportunities and Challenges," in IT Professional, vol. 22, no. 1, pp. 34-38, 2020.
[4] T. R. Raddo, et al., "Transition technologies towards 6G networks," Journal of Wireless Communications and Networking, vol. 100, pp. 1-22, 2021. https://doi.org/10.1186/s13638-021-01973-9 .
[5] N. Suzuki, H. Miura, "Digital Coherent DSP based PON Technology for Ultimate Capacity Optical Access Systems," 2020 IEEE Photonics Society Summer Topicals Meeting Series (SUM), 2020, pp. 1-2, 2020.
[6] "50-Gigabit-capable passive optical networks (50G-PON): Physical media dependent (PMD) layer specification," 2020.
[Online] https://www.itu.int/itu-t/workprog/wp_item.aspx?isn=14550
[7] V. Houtsma, A. Mahadevan, N. Kaneda, D. van Veen, "Transceiver technologies for passive optical networks: past, present, and future [Invited Tutorial]," J. Opt. Commun. Netw. 13, A44-A55, 2021.
[8] D. Zhang, D. Liu, X. Wu, D. Nesset, "Progress of ITU-T higher speed passive optical network (50G-PON) standardization," J. Opt. Commun. Netw. 12, D99-D108, 2020.
[9] J. S. Wey and J. Zhang, "Passive Optical Networks for 5G Transport: Technology and Standards," in Journal of Lightwave Technology, vol. 37, no. 12, pp. 2830-2837, 15 June15, 2019.
[10] T. Pfeiffer, "Next generation mobile fronthaul and midhaul architectures [Invited]," in IEEE/OSA Journal of Optical Communications and Networking, vol. 7, no. 11, pp. B38-B45, 2015
[11] J. S. Wey, Y. Luo and T. Pfeiffer, "5G Wireless Transport in a PON Context: An Overview," IEEE Communications Standards Magazine, vol. 4, no. 1, pp. 50-56, 2020
[12] R. Sabella, P. Iovanna, G. Bottari, F. Cavaliere, "Optical transport for Industry 4.0 [Invited]," J. Opt. Commun. Netw. 12, 264-276, 2020.
[13] D. van Veen, V. Houtsma, "Strategies for economical next-generation 50G and 100G passive optical networks [Invited]," J. Opt. Commun. Netw. 12, A95-A103, 2020.
[14] J. Zhang, J. Yu, J. Shan Wey, X. Li , Li Zhao, K. Wang, M. Kong, W. Zhou, J. Xiao, X. Xin, F. Zhao, "SOA Pre-Amplified 100 Gb/s/λ PAM-4 TDM-PON Downstream Transmission Using 10 Gbps O-Band Transmitters," J. Lightwave Technol., vol.38, pp. 185-193, 2020.
[15] S. Luo, Z. Li, Y. Qu, Y. Song, J. Chen, Y. Li, M. Wang, "112-Gb/s/λ Downstream Transmission for TDM-PON with 31-dB Power Budget using 25-Gb/s Optics and Simple DSP in ONU," in Proc. Optical Fiber Communication Conference (OFC), 2020, paper Th3K.4

[16] M. G. Saber, D. V. Plant, R. Gutiérrez-Castrejón, M. S. Alam, Z. Xing, E. El-Fiky, L. Xu, F. Cavaliere, G. Vall-Llosera, S. Lessard, "100 Gb/s/λ Duo-Binary PAM-4 Transmission Using 25G Components Achieving 50 km Reach," IEEE Photonics Technology Letters, vol. 32, no. 3, pp. 138-141, 2020.
[17] P. Torres-Ferrera, H. Wang, V. Ferrero, R. Gaudino, "100 Gbps/λ PON downstream O- and C-band alternatives using direct-detection and linear-impairment equalization [Invited]," J. Opt. Commun. Netw. 13, A111-A123, 2021.
[18] P. Torres-Ferrera, G. Rizzelli, V. Ferrero, R. Gaudino, "100+ Gbps/λ 50 km C-Band Downstream PON Using CD Digital Pre-Compensation and Direct-Detection ONU Receiver," J. Lightwave Technol. 38, 6807-6816, 2020.
[19] L. Yi, T. Liao, L. Huang, L. Xue, P. Li, W. Hu, "Machine Learning for 100 Gb/s/λ Passive Optical Network," J. Lightwave Technol. vol. 37, pp. 1621-1630, 2019.
[20] V. Houtsma, E. Chou, D. van Veen, "92 and 50 Gbps TDM-PON using Neural Network Enabled Receiver Equalization Specialized for PON," Proc. Optical Fiber Communication Conference (OFC), 2019, paper M2B.6.
[21] R. Borkowski et al., "World's First Field Trial of 100 Gbit/s Flexible PON (FLCS-PON)," European Conference on Optical Communications (ECOC), pp. 1-4, 2020.
[22] M. S. Erkılınç, R. Emmerich, K. Habel, V. Jungnickel, C. Schmidt-Langhorst, C. Schubert, and R. Freund, "PON transceiver technologies for ≥50 Gbits/s per λ: Alamouti coding and heterodyne detection [Invited]," J. Opt. Commun. Netw. 12, A162-A170, 2020.
[23] N. Suzuki, H. Miura, K. Matsuda, R. Matsumoto, K. Motoshima, "100 Gb/s to 1 Tb/s based coherent passive optical network technology," J. Lightw. Technol., vol. 36, no. 8, pp. 1485–1491, 2018.
[24] J. Zhang, J. Shan Wey, J. Shi, J. Yu, "Single-wavelength 100-Gb/s PAM-4 TDM-PON achieving over 32-dB power budget using simplified and phase insensitive coherent detection," in Proc. Eur. Conf. Opt. Commun. (ECOC), 2018, Paper Tu1B.1
[25] J. Zhang, Z. Jia, M. Xu, H. Zhang, L. A. Campos, "Efficient preamble design and digital signal processing in upstream burst-mode detection of 100G TDM coherent-PON," J. Opt. Commun. Netw. 13, A135-A143, 2021.
[26] R. Matsumoto, K. Matsuda, N. Suzuki, "Burst-Mode coherent detection using fast-fitting pilot sequence for 100-Gb/s/λ coherent TDM-PON systems," in Proc. Eur. Conf. Opt. Commun. (ECOC), 2017, Paper W.3.D.5
[27] K. Matsuda, R. Matsumoto, N. Suzuki, "Hardware-Efficient Adaptive Equalization and Carrier Phase Recovery for 100-Gb/s/λ-Based Coherent WDM-PON Systems," J. Lightwave Technol. 36, 1492-1497 (2018)
[28] Y. Zhu, L. Yi, B. Yang, X. Huang, J. Shan Wey, Z. Ma, W. Hu, "Comparative study of cost-effective coherent and direct detection schemes for 100 Gb/s/λ PON," J. Opt. Commun. Netw. 12, D36-D47, 2020.
[29] IEEE Standard for Ethernet Amendment 9: Physical Layer Specifications and Management Parameters for 25 Gb/s and 50 Gb/s Passive Optical Networks, in IEEE Std 802.3ca-2020, pp. 1-267, 2020.
[30] P. Torres-Ferrera, V. Ferrero, M. Valvo, R. Gaudino, "Impact of the Overall Electrical Filter Shaping in Next-Generation 25 and 50 Gb/s PONs", Journal of Optical Communications and Networking, vol. 10, no. 5, pp. 493-505, 2018.
[31] M. Tao, J. Zheng, X. Dong, K. Zhang, L. Zhou, H. Zeng, Y. Luo, S.Li, and X. Liu, "Improved dispersion tolerance for 50G-PON downstream transmission via receiver-side equalization," in Optical Fiber Communication Conference (OFC), paper M2B.3, 2019.
[32] Z. Zhang et al., "Optical- and Electrical-Domain Compensation Techniques for Next-Generation Passive Optical Networks," in IEEE Communications Magazine, vol. 57, no. 4, pp. 144-150, 2019.
[33] P. Torres-Ferrera, H. Wang, V. Ferrero, M. Valvo, R. Gaudino, "Optimization of Band-Limited DSP-Aided 25 and 50 Gb/s PON Using 10G-Class DML and APD," J. Lightwave Technol., vol. 38, pp. 608-618, 2020.
[34] L. A. Neto, J. Maes, P. Larsson-Edefors, J. Nakagawa, K. Onohara and S. J. Trowbridge, "Considerations on the Use of Digital Signal Processing in Future Optical Access Networks," in Journal of Lightwave Technology, vol. 38, no. 3, pp. 598-607, 2020.
[35] J. Zhang et al., "64-Gb/s/λ Downstream Transmission for PAM-4 TDMPON with Centralized DSP and 10G Low-Complexity Receiver in C-Band," European Conference on Optical Communication (ECOC), Gothenburg, pp. 1-3, 2017.
[36] R. Bonk, "SOA for future PONs," in Proc. Optical Fiber Communication Conference (OFC), 2018, paper Tu2B.4.
[37] T. Shindo, N. Fujiwara, S. Kanazawa, M. Nada, Y. Nakanishi, T. Yoshimatsu, A. Kanda, M. Chen, Y. Ohiso, K. Sano, H. Matsuzaki, "High Power and High Speed SOA Assisted Extended Reach EADFB Laser (AXEL) for 53-Gbaud PAM4 Fiber-Amplifier-Less 60-km Optical Link," J. Lightwave Technol. vol. 38, 2984-2991, 2020.

[38] E. Harstead, R. Bonk, S. Walklin, D. van Veen, V. Houtsma, N. Kaneda, A. Mahadevan, R. Borkowski, "From 25 Gb/s to 50 Gb/s TDM PON: transceiver architectures, their performance, standardization aspects, and cost modeling," *J. Opt. Commun. Netw.* 12, D17-D26, 2020.

[39] P. N. Goki, M. Imran, C. Porzi, V. Toccafondo, F. Fresi, F. Cavaliere, L. Potì, "Lossless WDM PON Photonic Integrated Receivers Including SOAs," *Appl. Sci.* 9, p. 2457, 2019.

[40] C. Caillaud *et al.*, "High sensitivity 40 Gbit/s preamplified SOA-PIN/TIA receiver module for high speed PON," *2014 The European Conference on Optical Communication (ECOC)*, 2014, pp. 1-3, doi: 10.1109/ECOC.2014.6963903.

[41] J. Prat, A. Napoli, J. M. Gené, M. Omella, P. Poggiolini, and V. Curri, "Square root strategy: A novel method to linearise an optical communications system with linear equalizers," in Proc. ECOC 2005, Glasgow, U.K., 2005, Paper We4.P.106

[42] J. Prat, M. C. Santos and M. Omella, "Square Root Module to Combat Dispersion-Induced Nonlinear Distortion in Radio-Over-Fiber Systems," in IEEE Photonics Technology Letters, vol. 18, no. 18, pp. 1928-1930, Sept.15, 2006.

[43] D. Nesset, "NG-PON2 Technology and Standards," in Journal of Lightwave Technology, vol. 33, no. 5, pp. 1136-1143, 2015.

[44] D. Zhang, D. Zhe, M. Jiang, and J. Zhang, "High speed WDM-PON technology for 5G fronthaul network," Asia Communications and Photonics Conference (ACP), paper S3K.8, 2018.

[45] A. Rashidinejad, A. Nguyen, M. Olson, S. Hand and D. Welch, "Real-Time Demonstration of 2.4Tbps (200Gbps/λ) Bidirectional Coherent DWDM-PON Enabled by Coherent Nyquist Subcarriers," Optical Fiber Communications Conference and Exhibition (OFC), pp.1-3, 2020

[46] W. Saad, M. Bennis and M. Chen, "A Vision of 6G Wireless Systems: Applications, Trends, Technologies, and Open Research Problems," in *IEEE Network*, vol. 34, no. 3, pp. 134-142, 2020.

[47] X. Chen, S. Chandrasekhar and P. Winzer, "Self-coherent systems for short reach transmission," Proc. Eur. Conf. Opt. Commun., pp. 1-3, 2018.

[48] X. Chen, C. Antonelli, S. Chandrasekhar, G. Raybon, A. Mecozzi, M. Shtaif, P. Winzer, "Kramers–Kronig Receivers for 100-km Datacenter Interconnects," J. Lightwave Technology, 36, pp. 79-89, 2018.

[49] S. T. Le, K. Schuh, R. Dischler, F. Buchali, L. Schmalen and H. Buelow, "Beyond 400 Gb/s Direct Detection Over 80 km for Data Center Interconnect Applications," *J. Lightwave Technol*, vol. 38, no. 2, pp. 538-545, 2020.

[50] IEEE 802.3 Physical Layers for increased-reach Ethernet optical subscriber access (Super-PON) Study Group, 2018.

[51] C. DeSanti, L. Du, J. Guarin, J. Bone, C. F. Lam, "Super-PON: an evolution for access networks [Invited]," J. Opt. Commun. Netw. 12, D66-D77, 2020.

[52] L. B. Du *et al.*, "Long-Reach Wavelength-Routed TWDM PON: Technology and Deployment," J. Lightw. Technol., 37(3), pp.688-697, 2019.

[53] D. Lavery, R. Maher, D. S. Millar, B. C. Thomsen, P. Bayvel, S. J. Savory, "Digital Coherent Receivers for Long-Reach Optical Access Networks," *Journal of Lightwave Technology*, 31, 609-620, 2013.

[54] H. Wang, P. Torres-Ferrera, G. Rizzelli, V. Ferrero, R. Gaudino "100 Gbps/λ C-band CD Digital Pre-compensated and Direct-Detection Links with Simple Non-Linear Compensation," IEEE Photonics Journal, vol. 13, no. 4, pp. 1-8, 2021.

[55] J. Tsimbinos, K. V. Lever, "The computational complexity of nonlinear compensators based on the Volterra inverse," Proceedings of 8th Workshop on Statistical Signal and Array Processing, pp. 387-390, 1996

Pablo Torres-Ferrera received the B.Eng., M.E.E. and Ph.D. degrees (with honors) in telecommunications in 2010, 2012 and 2017, respectively, from the National Autonomous University of Mexico (UNAM), Mexico City. He worked from 2012 to 2013 at Huawei Technologies Mexico in the implementation of OTN rings. As part of his PhD investigation work, he carried out research internships at Athens Information Technology (AIT), Greece, in 2014 and at Politecnico di Torino, Italy, in 2016. Since 2017, he is a Researcher at Politecnico di Torino, working in the field of high-speed optical access networks and data-center interconnects.

Giuseppe Rizzelli is Assistant Professor at the Department of Electronics and Telecommunications of Politecnico di Torino, Italy. He received his PhD in Electronics Engineering from Alcalá University (Madrid, Spain) in 2018, where he worked on distributed Raman amplification for both, long-haul and unrepeated optical communications. Prior to enrolling in the PhD program, he was affiliate researcher at the Lawrence Berkeley National Laboratory (CA, USA) where he worked on mode-locked lasers synchronization. He recently joined the Optcom group at Politecnico di Torino where his main research focus is on short-reach optical communications both for metro access and datacenter scenarios.

Haoyi Wang received the bachelor degree in Telecommunication Engineering in 2015, and the master degree in Communication and Computer Networks Engineering in 2018, both from Politecnico di Torino, Italy. Now, she is a Ph.D. candidate in Electrical, Electronics and Communication Engineering at Politecnico di Torino. Her current research is in the field of high-speed optical access networks.

Valter Ferrero (M'97) received the Laurea degree (summa cum laude) in Electronics Engineering in 1994 from Politecnico di Torino, Italy. In 1994, he collaborated with Politecnico di Torino, working on coherent optical systems. From 1995 to 1996, he was with GEC Marconi (now Ericson), Genova, Italy. In 1997, he joined the Optical Laboratory, Department of Electrical Engineering, Politecnico di Torino. He is currently Associate Professor at Politecnico di Torino. He is author or co-author of more than 90 papers in the field of Optical Communications. His current research interests include optical coherent communications, free-space optical communications, and next-generation passive optical networks.

Roberto Gaudino Ph.D., is currently Full Professor at Politecnico di Torino, Italy. His main research interests are in the long haul DWDM systems, fiber non-linearity, modelling of optical communication systems and in the experimental implementation of optical networks, with specific focus on access networks. In particular, in the last five years, he focused his activity on short-reach optical links using plastic optical fibers (POF) and on next-generation passive optical access networks (NG-PON2). Currently, he is working on ultra-high capacity systems for medium reach links. Previously, he worked extensively on fiber modelling, optical modulation formats, coherent optical detection, and on the experimental demonstration of packet switched optical networks. He is author or co-author of more than 200 papers in the field of Optical Communications. From 2009 to 2016 he was the coordinator of three projects in the area of optical access (EU FP6-IST STREP "POF-ALL" and "POF-PLUS" and EU FP7-ICT STREP project "FABULOUS"). He is now the coordinator of the PhotoNext center at POLITO.